

---

# Uncertainty-aware Accumulated Local Effects (UALE) for quantifying the heterogeneity of instance-level feature effects

---

Anonymous Author  
Anonymous Institution

## Abstract

Accumulated Local Effects (ALE) is a popular approach to explainable AI that quantifies how a feature influences the decisions of a model taking into account feature correlations. However, in case of strong interactions between features, instance-level feature effects may deviate from the average curve provided by ALE. Therefore, it is crucial to quantify this deviation, namely, the uncertainty of the effect. In this work, we define Uncertainty-aware ALE (UALE) to quantify and visualize, on a single plot, both the average effect and the uncertainty. Furthermore, as in ALE, UALE’s approximation requires partitioning the feature domain into non-overlapping intervals (bin-splitting). The average effect and the uncertainty are then computed from the instances that lie in each bin. In this work, we formally prove that to achieve an unbiased approximation of the uncertainty in each bin, bin-splitting must follow specific constraints. Based on this, we propose a method for automatically finding the optimal intervals, balancing the trade-off between estimation bias and variance [check if this phrase explains well the concept.] We demonstrate through synthetic and real datasets (a) the advantages of modeling the uncertainty with UALE compared to other methods and (b) the importance of appropriate bin splitting for an accurate approximation of the average effect and uncertainty.

## 1 INTRODUCTION

Recently, Machine Learning (ML) has been adopted in critical domains, such as healthcare and finance. In these ar-

eas, we need a combination of accurate predictions along with meaningful explanations to support them. For this reason, there is an increased interest in Explainable AI (XAI) to understand the decision mechanism of complex black-box models. XAI literature distinguishes between local and global techniques (Molnar et al., 2020a). Local methods provide instance-level explanations, i.e. explain the prediction for a specific instance, whereas global methods summarize the entire model behavior.

Global methods create a global explanation by aggregating the instance-level explanations into a single interpretable outcome, usually a number or a plot. A popular class of global methods are the so-called Feature Effect (FE) methods (Grömping, 2020) that isolate the impact of a single feature on the output<sup>1</sup>. There are three widely-used FE methods: *Partial Dependence Plots* (PDP)(Friedman, 2001), *Marginal Plots* (MP)(Apley and Zhu, 2020) and *Aggregated Local Effects* (ALE)(Apley and Zhu, 2020) with ALE being established as the state-of-the-art for measuring the average effect, since PDP and MP have been criticized (Grömping, 2020) to compute erroneous effects when the input features are (highly) correlated.

However, when strong interactions between features exist, the instance-level feature effects may significantly deviate from the aggregated outcome of ALE (Herbinger et al., 2022), a phenomenon called *aggregation bias* (Mehrabian et al., 2021). Aggregation bias leads to ambiguities; for example, a feature with zero average effect may indicate no effect on the output or a highly positive effect for some instances and a highly negative effect for others. Such ambiguities could be resolved if not only the average effect but also the deviation of instance-level feature effects, a quantity we refer to as the *uncertainty of the effect*, from the average effect is provided.

In this work, we propose UALE, a global feature-effect method that extends ALE by quantifying the uncertainty associated with the average effect. Similarly to ALE, UALE’s approximation requires partitioning the feature do-

---

Preliminary work. Under review by AISTATS 2023. Do not distribute.

---

<sup>1</sup>FE methods also isolate the combined effect of a pair of features to the output. Combinations of more than two features are uncommon, since they are difficult to estimate and visualize.

main into non-overlapping intervals (bin-splitting). However, as we formally prove, a fixed equi-width partitioning without considering the characteristics of the instance-level effects may lead to an erroneous (biased) estimation of the uncertainty. Therefore, we propose an automatic uncertainty-driven partitioning that secures an unbiased approximation of the uncertainty.

[This should go to related work]In contrast, in PDP the heterogeneity of instance-level effects can be identified by exploring the Individual Conditional Expectations (ICE) (Goldstein et al., 2015). [to be moved in related work] Finding an appropriate sequence of bins is of particular importance, since ALE’s interpretation is meaningful only inside each bin (Molnar, 2022). However, this crucial step has not raised the appropriate attention. With the current approaches (Apley and Zhu, 2020; Gkolemis et al.), the domain is split *blindly*, i.e. without considering the characteristics of the instance-level effects, in  $K$  equi-sized bins.

The contributions of this paper are:

- A global feature effect method that quantifies both the average effect and the uncertainty, i.e., the heterogeneity of instance level effects.
- An unbiased approximation of the uncertainty through a dynamic uncertainty-driven bin partitioning of the feature domain.
- A thorough evaluation on both synthetic and real datasets.

The implementation of our method and the code for reproducing all the experiments is provided in the submission and will become publicly available upon acceptance.

## 2 BACKGROUND AND RELATED WORK

We here review the existing methods for modeling the average effect and the heterogeneity of instance-level effects. The necessary background for ALE (Apley and Zhu, 2020) is presented in Section 2.1, whereas ALE approximations (Apley and Zhu, 2020; Gkolemis et al.) are presented in Section 2.3.

**Notation** Let  $\mathcal{X} \in \mathbb{R}^d$  be the  $d$ -dimensional feature space,  $\mathcal{Y} \in \mathbb{R}$  the target space and  $f(\cdot) : \mathcal{X} \rightarrow \mathcal{Y}$  the black-box function. We use index  $s \in \{1, \dots, d\}$  for the feature of interest and  $c \in \{1, \dots, d\} - s$  for the rest feature indexes. For convenience, we denote the feature vector  $\mathbf{x} = (x_1, \dots, x_s, \dots, x_D)$  with  $(x_s, \mathbf{x}_c)$  and the corresponding random variables  $X = (X_1, \dots, X_s, \dots, X_D)$  with  $(X_s, X_c)$ . The training set is  $\mathcal{D} = \{(\mathbf{x}^i, y^i)\}_{i=1}^N$

sampled i.i.d. from the distribution  $\mathbb{P}_{X,Y}$ . Finally, we use  $f^{\langle \text{method} \rangle}(x_s)$  for the FE of the  $s$ -th feature, with  $\langle \text{method} \rangle$  indicating the particular method in use, for example ALE.<sup>2</sup>

### 2.1 Feature Effect Methods and ALE

The three well-known feature effect methods are: *Partial Dependence Plots* (PDP)(Friedman, 2001), *Marginal Plots* (MP)(Apley and Zhu, 2020) and *Aggregated Local Effects* (ALE)(Apley and Zhu, 2020) PDP formulates the FE of the  $s$ -th attribute as an expectation over the origin/overleaf-2022-10-11-1029 marginal distribution  $\mathbf{X}_c$ , i.e.,  $f^{\text{PDP}}(x_s) = \mathbb{E}_{\mathbf{X}_c}[f(x_s, \mathbf{X}_c)]$ , whereas MP formulates it as an expectation over the conditional  $\mathbf{X}_c|X_s$ , i.e.,  $f^{\text{MP}}(x_s) = \mathbb{E}_{\mathbf{X}_c|X_s}[f(x_s, \mathbf{X}_c)]$ . ALE defines the local effect of the  $s$ -th feature at instance  $x_s = z$  as  $f^s(z, \mathbf{x}_c) = \frac{\partial f}{\partial x_s}(z, \mathbf{x}_c)$ . All the local explanations at  $z$  are, then, weighted by the conditional distribution  $p(\mathbf{x}_c|x_s = z)$  and are averaged, to produce the averaged effect  $\mu(z)$ . ALE is the accumulation of the averaged local effects:

$$f^{\text{ALE}}(x_s) = \int_{x_{s,\min}}^{x_s} \underbrace{\mathbb{E}_{\mathbf{X}_c|X_s=z}[f^s(z, \mathbf{X}_c)]}_{\mu(z)} dz \quad (1)$$

Eq. (1) has specific advantages which gain particular value in cases of correlated input features. In these cases, PDP integrates over unrealistic instances due to the use of the marginal distribution  $\mathbf{X}_c$ , and MP computes aggregated effects, i.e., imputes the combined effect of sets of features to a single feature. ALE manages to resolve both issues, and is therefore the most trustable method in cases of correlated features. [cite someone]

### 2.2 Heterogeneity Of Instance-Level Effects

iiiiiii HEAD FE methods show what is the average (global) effect on the output, if the value of a specific feature is increased/decreased. For completing the explanation about a feature, we need to also know to what extent the local effects [add what local means here] deviate from the global explanation, i.e. to quantify the uncertainty of the average effect. [A connector line is needed here on the connection between local-global and uncertainty] ICE and d-ICE(Goldstein et al., 2015) provide a set of curves that are plot on top-of PDP. Both methods produce one curve for each instance of the training set;  $f_i^{\text{ICE}}(x_s) = f(x_s, \mathbf{x}_c^i)$  for ICE and  $f_i^{\text{d-ICE}}(x_s) = \frac{\partial f}{\partial x_s}(x_s, \mathbf{x}_c^i)$  for d-ICE. The user then visually observes if the curves are homogeneous, i.e., all instances have similar values, and to what extent they deviate from the PDP. Some methods try to automate the aforementioned visual exploration, by grouping

<sup>2</sup>An extensive list of all symbols used in the paper is provided at the Appendix.

(d-)ICE plots into clusters (Molnar et al., 2020b; Herbringer et al., 2022; Britton, 2019). Other approaches, like H-Statistic (Friedman and Popescu, 2008), Greenwell’s interaction index (Greenwell et al., 2018) or SHAP interaction ||||| HEAD values (Lundberg et al., 2018) inform indirectly about heterogeneous effects, quantifying interactions between the input features. A strong interaction index is an indicator for the existence of heterogeneous effects.

The aforementioned approaches are under two limitations. They either do not quantify the uncertainty of the FE directly [I dont get this argument. What do you mean directly?] or they are based

on PDPs, and, therefore, they are subject to the failure modes of PDPs in cases of correlated features (Baniecki et al., 2021), as we will also show in our experimental analysis (c.f., Section 4.1). To the best of our knowledge, no work exist so far that quantifies the heterogeneous effects based on the formulation of ALE. [My understanding of the contribution is also the last sentence. None has done it for ALE, but it has been done f for PDPs. For this I think we need some more related owrk on the limiations of PDPs. Also, is this work a straight-forward transfer of the d-ICE etc methods decribed above or transferring these ideas to ALE requires a different approach?]

### 2.3 ALE Approximation

||||| HEAD In ML scenarios, ALE is estimated from the instances of the training set. (Apley and Zhu, 2020) proposed dividing the feature domain in  $K$  equisized bins and estimating the local effects in each bin by evaluating the black box-function  $f$  at the bin limits: [k or K? I prefer k for the cardinality and it seems that k is used afterwards. ]

$$\hat{f}^{\text{ALE}}(x_s) = \sum_{k=1}^{k_x} \frac{1}{|\mathcal{S}_k|} \sum_{i: \mathbf{x}^i \in \mathcal{S}_k} [f(z_k, \mathbf{x}_c^i) - f(z_{k-1}, \mathbf{x}_c^i)] \quad (2)$$

We denote as  $k_x$  the index of the bin that  $x_s$  belongs to, i.e.  $k_x : z_{k_x-1} \leq x_s < z_{k_x}$  and  $\mathcal{S}_k$  is the set of training instances of the  $k$ -th bin, i.e.  $\mathcal{S}_k = \{\mathbf{x}^i : z_{k-1} \leq x_s^i < z_k\}$ .

(Gkolemis et al.) proposed the Differential ALE (DALE) that computes the local effects on the training instances using auto-differentiation:

$$\hat{f}^{\text{DALE}}(x_s) = \Delta x \sum_{k=1}^{k_x} \frac{1}{|\mathcal{S}_k|} \sum_{i: \mathbf{x}^i \in \mathcal{S}_k} f^s(\mathbf{x}^i) \quad (3)$$

Their method has the advantages of remaining on-distribution even when bins become wider and, most importantly, allows the recomputation of the accumulated effect with different bin-splitting with near-zero additional computational cost.

Both approximations, however, require the number of bins  $K$  as input and perform an equally-sized bin splitting of the attribute domain. The choice of  $K$  is therefore critical and introduces significant limitations. Specifically, setting  $K$  to a small value may hide fine-grain effects due to large bins while setting  $K$  to a high value leads to poor bin-effect estimations due to few samples per bin. In general, the user may receive contradictory explanations for different  $K$  values without a clue for which one to trust.

## 3 Uncertainty-Aware ALE (UALE)

UALE extends ALE for quantifying the level of heterogeneous effects (uncertainty) and automates the bin-splitting. At Section 3.1 we define UALE, at Section 3.2 we reformulate it using an interval-based formulation, at Section 3.3 we provide UALE approximation and at Section 3.4 we define and solve the problem of optimal bin-splitting.

### 3.1 UALE: ALE With Uncertainty Quantification

UALE extends ALE definition of Eq. (1) with a component for quantifying the uncertainty. We denote as  $\mathcal{H}(z)$  the uncertainty of the local effects at a specific point  $x_s = z$  and we quantify it with the standard deviation of the local explanations  $\mathcal{H}(z) = \sigma(z)$ , where:

$$\sigma^2(z) = \mathbb{E}_{\mathbf{x}_c|z} [(f^s(z, X_c) - \mu(z))^2] \quad (4)$$

The uncertainty emerges from the natural characteristics of the experiment, i.e., the feature correlations existent in the data generating distribution and the implicit interactions of the black-box function. We also define the accumulated uncertainty at  $x_s$ , as the accumulation of the standard deviation of the local effects along the axis:

$$f_{\sigma}^{\text{ALE}}(x_s) = \int_{x_{s,\min}}^{x_s} \sigma(z) \partial z \quad (5)$$

UALE formulates the effect at a specific point  $x_s$  with a tuple that consists of the average effect and the uncertainty  $(\mu(z), \sigma(z))$  and visualizes it with a continuous curve and a confidence region  $f^{\text{UALE}}(x_s) := f_{\mu}^{\text{ALE}}(x_s) \pm f_{\sigma}^{\text{ALE}}(x_s)$ .

### 3.2 Interval-Based Formulation and Approximation

In real ML scenarios, all estimations are based on the instances of the training set. Therefore, we cannot estimate  $\mu(z), \sigma(z)$  at the granularity of a point, because the probability of observing a sample inside the region  $[x_s - h, x_s + h]$  tends to zero, when  $h \rightarrow 0$ . We define the regional-effect  $\mu(z_1, z_2)$  and the regional-uncertainty  $\mathcal{H}(z_1, z_2) = \sigma(z_1, z_2)$ , as the summary statistics that characterize the effect and the uncertainty inside the interval  $[z_1, z_2]$ :

$$\mu(z_1, z_2) = \mathbb{E}_{z \sim \mathcal{U}(z_1, z_2)}[\mu(z)] = \frac{\int_{z_1}^{z_2} \mu(z) \partial z}{z_2 - z_1} \quad (6)$$

$$\sigma^2(z_1, z_2) = \mathbb{E}_{z \sim \mathcal{U}(z_1, z_2)}[\sigma^2(z)] = \frac{\int_{z_1}^{z_2} \sigma^2(z) \partial z}{z_2 - z_1} \quad (7)$$

Intuitively, the regional-effect and the regional-uncertainty quantify the expected average effect and the expected uncertainty if we randomly draw a point  $z^*$  given a uniform distribution  $z^* \sim \mathcal{U}(z_1, z_2)$ . If we also define as  $\mathcal{Z}$  the sequence of  $K + 1$  points that partition the domain of the  $s$ -th feature into  $K$  variable-size intervals, i.e.  $\mathcal{Z} = \{z_0, \dots, z_K\}$ , we can redefine UALE using an interval-based formulation  $\tilde{f}_{\mathcal{Z}}^{\text{UALE}}(x_s) := \tilde{f}_{\mathcal{Z}, \mu}^{\text{ALE}}(x_s) \pm \tilde{f}_{\mathcal{Z}, \sigma}^{\text{ALE}}(x_s)$ , where:

$$\tilde{f}_{\mathcal{Z}, \mu}^{\text{ALE}}(x_s) = \sum_{k=1}^{k_x} \mu(z_{k-1}, z_k)(z_k - z_{k-1}) \quad (8)$$

$$\tilde{f}_{\mathcal{Z}, \sigma}^{\text{ALE}}(x_s) = \sum_{k=1}^{k_x} \sigma(z_{k-1}, z_k)(z_k - z_{k-1}) \quad (9)$$

### 3.3 Interval-Based Approximation

For approximating the mean effect (Eq. (6)) and the uncertainty (Eq. (7)) we use the set  $\mathcal{S}_k$  of dataset instances with the  $s$ -th feature lying inside the interval  $\mathcal{S}_k = \{\mathbf{x}^i : z_{k-1} \leq x_s^i < z_k\}$ :

$$\hat{\mu}(z_{k-1}, z_k) = \frac{1}{|\mathcal{S}_k|} \sum_{i: \mathbf{x}^i \in \mathcal{S}_k} [f^s(\mathbf{x}^i)] \quad (10)$$

$$\hat{\sigma}^2(z_{k-1}, z_k) = \frac{1}{|\mathcal{S}_k|} \sum_{i: \mathbf{x}^i \in \mathcal{S}_k} (f^s(\mathbf{x}^i) - \hat{\mu}(z_1, z_2))^2 \quad (11)$$

Eq.(10) is an unbiased estimator of Eq. (6) under the assumption that the points are uniformly distributed inside the intervals. The same does not hold in the general case for Eq.(11). In the general case,  $\hat{\sigma}^2(z_{k-1}, z_k)$  is an unbiased estimator of the *observable* variance  $\sigma_{obs}^2(z_1, z_2) = \frac{\int_{z_1}^{z_2} \mathbb{E}_{\mathbf{x}_c | x_s = z} [(f^s(z, \mathbf{x}_c) - \mu(z_1, z_2))^2] \partial z}{z_2 - z_1}$ , which as we prove in Theorem 1 is an overestimation of  $\sigma^2(z_1, z_2)$ .

**Theorem 1.** *If we define the residual  $\rho(z)$  as the difference between the expected effect at  $x_s$  and the regional effect, i.e  $\rho(z) = \mu(z) - \mu(z_1, z_2)$ , then the regional variance  $\sigma^2(z_1, z_2)$  equals to:*

$$\sigma_{obs}^2(z_1, z_2) = \sigma^2(z_1, z_2) + \frac{\int_{z_1}^{z_2} \rho^2(z) \partial z}{z_2 - z_1} \quad (12)$$

Theorem 1 reveals an important connection between the ground-truth and the observable uncertainty inside a region.

For convenience, we denote as  $\mathcal{E}^2(z_1, z_2) = \frac{\int_{z_1}^{z_2} \rho^2(z) \partial z}{z_2 - z_1}$  the error term that models the expected square residual inside the interval and as  $\mathcal{H}_{obs}(z_1, z_2) := \sigma_{obs}^2(z_1, z_2)$  the observable uncertainty. It holds that the observable uncertainty is an overestimation of the correct uncertainty

$$\mathcal{H}_{obs}^2(z_1, z_2) = \mathcal{H}^2(z_1, z_2) + \mathcal{E}^2(z_1, z_2) \quad (13)$$

and, therefore, the estimation is unbiased only in case  $\mathcal{E}^2(z_1, z_2) = 0$ .

### 3.4 Bin-Splitting: Finding Regions With Homogeneous Effects

In this section we formulate bin-splitting as an unsupervised clustering problem, searching for a solution that compromises two contradictory objectives. On the one hand, we want to minimize the error term  $\mathcal{E}$  for approaching an unbiased estimation and on the other hand, we want wide-enough bins for including a fair population of samples for a robust estimation of  $\hat{\mu}(z_1, z_2), \hat{\sigma}(z_1, z_2)$ . We set-up the following optimization problem:

$$\begin{aligned} \min_{\mathcal{Z} = \{z_0, \dots, z_K\}} \quad & \mathcal{L} = \sum_{k=1}^K \tau_k \hat{\sigma}^2(z_{k-1}, z_k) \Delta z_k \\ \text{where} \quad & \Delta z_k = z_k - z_{k-1} \\ & \tau_k = 1 - \alpha \frac{|\mathcal{S}_k|}{N} \\ \text{s.t.} \quad & |\mathcal{S}_k| \geq N_{\text{NPB}} \\ & z_0 = x_{s, \min} \\ & z_K = x_{s, \max} \end{aligned} \quad (14)$$

We search for the sequence of intervals  $z_0, \dots, z_K$  that minimizes the sum of the bin costs. The cost of each bin is the approximated variance  $\hat{\sigma}_k^2$  scaled by the bin length  $\Delta z_k$  and discounted by the term  $\tau_k$ . The term  $\tau_k$  favors the selection of a bigger bin in case it has similar variance with the aggregate variance of many smaller ones. The constraint of at least  $N_{\text{NPB}}$  points per bin sets the lowest-limit for a *robust* estimation. The user can choose to what extent they favor the creation of wide bins through the discount parameter by setting the parameter  $\alpha$  and where they set the minimum for robust approximation with the parameter  $N_{\text{NPB}}$ . For providing a rough idea, in our experiments we set  $\alpha = 0.2$  which means that the discount ranges between  $[0\%, 20\%]$  and  $N_{\text{NPB}} = \frac{N}{20}$ . It is also important to clarify that by minimizing  $\hat{\sigma}_k^2 \approx \mathcal{H}_{obs}^2$ , we actually minimize the squared error term  $\mathcal{E}^2$ , since the term  $\mathcal{H}_{true}^2$  is independent of the bin splitting.

### 3.4.1 Solve Bin-Splitting with Dynamic Programming

[Review all the description] For achieving a computationally-grounded solution we set a threshold  $K_{max}$  on the maximum number of bins which also discretizes the solution space. The width of the bin can take discrete values that are multiple of the minimum step  $u = \frac{x_{s,max} - x_{s,min}}{K_{max}}$ . For defining the solution, we use two indexes. The index  $i \in \{0, \dots, K_{max}\}$  denotes the point ( $z_i$ ) and the index  $j \in \{0, \dots, K_{max}\}$  denotes the position of the  $j$ -th multiple of the minimum step, i.e.,  $x_j = x_{s,min} + j \cdot u$ . The recursive cost function  $T(i, j)$  is the cost of setting  $z_i = x_j$ :

$$\mathcal{T}(i, j) = \min_{l \in \{0, \dots, K_{max}\}} [\mathcal{T}(i-1, l) + \mathcal{B}(x_l, x_j)] \quad (15)$$

where  $\mathcal{T}(0, j)$  equals zero if  $j = 0$  and  $\infty$  in any other case.  $\mathcal{B}(x_l, x_j)$  denotes the cost of creating a bin with limits  $[x_l, x_j]$ :

$$\mathcal{B}(x_l, x_j) = \begin{cases} \infty, & \text{if } x_j > x_l \text{ or } |\mathcal{S}_{(x_j, x_l)}| < N \\ 0, & \text{if } x_j = x_l \\ \hat{\sigma}^2(x_j, x_l), & \text{if } x_j \leq x_l \end{cases} \quad (16)$$

The optimal solution is given by solving  $\mathcal{L} = \mathcal{T}(K_{max}, K_{max})$  and keeping track of the sequence of steps.

- Discuss more aspects (e.g. Computational complexity)

## 4 SIMULATION EXAMPLES

In XAI it is common (Aas et al., 2021; Herbringer et al., 2022) to use simulation examples for comparing methods, because the data-generating distribution  $p(\mathbf{X})$  and the predictive function  $f(\cdot)$  are known, and, therefore, the ground-truth is accessible. We follow this common XAI practice and we split the evaluation in two groups of examples. The first group (Section 4.1) compares UALE definition against PDP-ICE in modeling the average effect and the uncertainty. The second group (Section 4.2) compares UALE approximation using the automatic bin-splitting against the fixed-size alternative, in estimating the average effect and the uncertainty.

### 4.1 Case 1: UALE vs PDP-ICE

In this simulation, we compare UALE against PDP-ICE. The aim of this example is to highlight that when features are correlated, PDP and ICE fail in quantifying the average effect and the heterogeneity, even when the black-box function is relatively simple.

We use the following distribution:  $p(\mathbf{x}) = p(x_3)p(x_2|x_1)p(x_1)$  where  $x_1 \sim \mathcal{U}(0, 1)$ ,  $x_2 = x_1$  and  $x_3 \sim \mathcal{N}(0, \sigma_3^2)$  and the following piecewise linear function:

$$f(\mathbf{x}) = \begin{cases} f_{lin} + \alpha f_{int} & \text{if } f_{lin} < 0.5 \\ 0.5 - f_{lin} + \alpha f_{int} & \text{if } 0.5 \leq f_{lin} < 1 \\ \alpha f_{int} & \text{otherwise} \end{cases} \quad (17)$$

where  $f_{lin}(\mathbf{x}) = a_1 x_1 + a_2 x_2$  and  $f_{int}(\mathbf{x}) = x_1 x_3$ . The linear term  $f_{lin}$  includes the two correlated features and the interaction term  $f_{int}$  the two non-correlated. We evaluate the effect computed by UALE and PDP-ICE in three cases; (a) without interaction ( $\alpha = 0$ ) and equal weights ( $a_1 = a_2$ ), (b) without interaction ( $\alpha = 0$ ) and different weights ( $a_1 \neq a_2$ ) and (c) with interaction ( $\alpha \neq 0$ ) with equal weights ( $a_1 = a_2$ ). In all cases, we provide the ground-truth average effect and uncertainty computed with analytical derivations (proofs at the Appendix) and we compare it against the approximations provided by each method, after generating  $N = 500$  samples.

**No Interaction, Equal weights.** In this set-up,  $\alpha = 0$  (no interaction) and the  $a_1 = a_2 = 1$  (equal weights). The ground truth effect  $f_{\mu}^{GT}(x_1)$  is:  $x_1$  in  $[0, 0.25]$ ,  $-x_1$  in  $[0.25, 0.5]$  and 0 in  $[0.5, 1]$ . The uncertainty is  $f_{\sigma^2}^{GT}(x_1) = 0$  in  $[0, 1]$  because  $x_1$  does not interact with other variables. In Figure 1, we observe that PDP effect is wrong and ICE plots imply the existence of heterogeneous effects. In contrast, UALE models correctly both the average effect and the zero uncertainty and approximates it accurately finding a zero aggregate residual error partitioning of  $x_1$  domain.

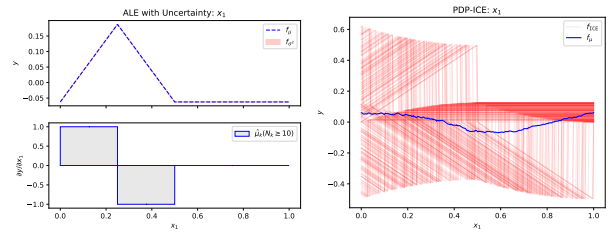


Figure 1: No interaction, Equal weights: Feature effect for  $x_1$  using UALE (Left) and PDP-ICE (Right).

**No Interaction, Non-Equal Weights.** In this set-up,  $\alpha = 0$  (no interaction),  $a_1 = 2$  and  $a_2 = 0.5$  (non-equal weights). The non-equal weights have implications at both the gradient and the interval of the piece-wise linear regions, i.e.,  $f_{\mu}^{GT}(x_1)$  is:  $2x_1$  in  $[0, 0.2]$ ,  $-2x_1$  in  $[0.2, 0.4]$  and 0 in  $[0.4, 1]$ . As before, the ground-truth uncertainty is  $f_{\sigma^2}^{GT}(x_1) = 0$  because  $x_1$  does not interact with other features. In Figure 2, we observe that PDP estimation is completely opposite to the ground-truth effect, i.e. negative in



the region  $[0, 0.2)$ , positive in  $[0.2, 0.4)$ , and the ICE erroneously implies the existence of heterogeneous effects. As before, ALE quantifies correctly the ground truth effect, the zero-uncertainty and partitioning correctly the  $x_1$  domain.

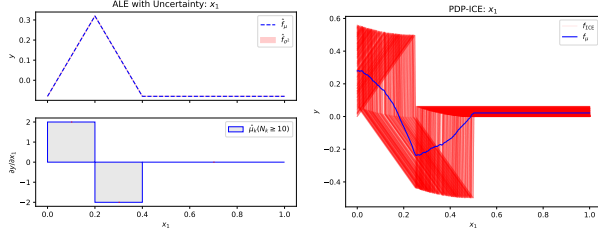


Figure 2: No interaction, Different weights: Feature effect for  $x_1$  using UALE (Left) and PDP-ICE (Right).

**Uncertainty, Equal weights.** In this set-up, we activate the interaction term, i.e.  $a = 1$ , keeping the weights equal  $a_1 = a_2 = 1$ . The interaction term provokes heterogeneous effects for features  $x_1$  and  $x_3$ , because the local effects at  $x_1$  depend on the unknown value of  $X_3$  and vice-versa. The effect of  $x_2$  has zero-uncertainty since it does not appear in any interaction term. As we observe in Figure 3, UALE correctly models the average effect and the uncertainty in all cases. On the other hand, PDP-ICE quantifies correctly the average effect and the uncertainty only in the case of feature  $x_3$ , because  $X_3$  is independent from other features. For the correlated features  $(x_1, x_2)$  both the average effect (PDP) and the uncertainty (ICE) are wrong.

**Discussion.** Despite the model’s simplicity, PDP-ICE fail in modeling both the average effect and the uncertainty. The error is due to the method’s formulation, i.e. the use of the marginal distribution that ignores correlations between features, and not due to poor approximation because of limited samples. In contrast, UALE models both correctly and estimates them accurately extracting the regions with constant effect. The examples above do not cover the case of an interaction term between correlated features, for example a term  $x_1x_2$ , because there is an open debate about the ground-truth effect in this case (Grömping, 2020).

## 4.2 Case 2: Bin-Splitting

In this simulation, we illustrate the advantages of automatic bin-splitting against the fixed-size alternative. For this reason, we generate a very big dataset applying dense sampling ( $N = 10^6$ ) and we treat the estimation with dense fixed-size bins ( $K = 10^3$ ) as the ground-truth UALE. Afterwards, we generate less samples ( $N = 500$ ) and we compare the fixed-size estimation (for many different  $K$ ) against UALE automatic bin-splitting. In all set-ups, we sample from  $p(\mathbf{x}) = p(x_2|x_1)p(x_1)$  where  $x_1 \sim \mathcal{U}(0, 1)$  and  $x_2 \sim \mathcal{N}(x_1, \sigma_2^2 = 0.5)$ . We denote as  $\mathcal{Z}^{\text{DP}} =$

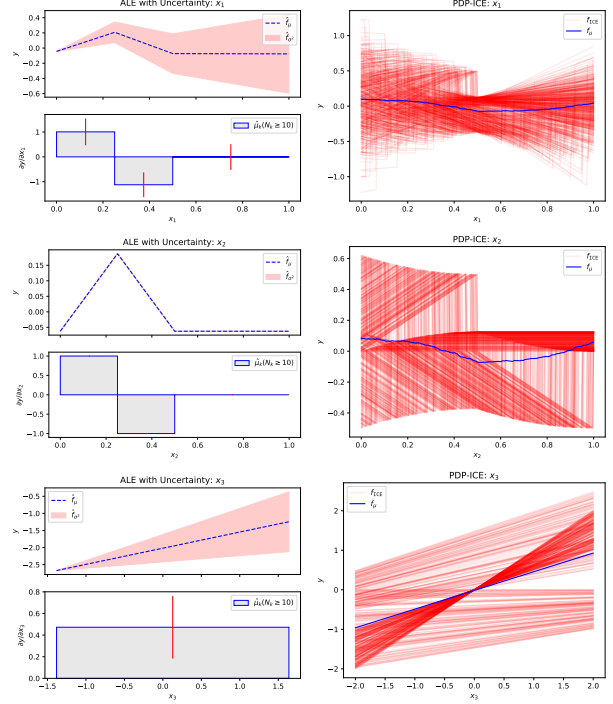


Figure 3: With interaction, equal weights: From top to bottom, feature effect for features  $\{x_1, x_2, x_3\}$  using UALE (left column) and PDP-ICE (right column).

$\{z_{k-1}^{\text{DP}}, \dots, z_K^{\text{DP}}\}$  the sequence obtained by automatic bin-splitting and with  $\mathcal{Z}^{\text{K}}$  the fixed-size splitting with  $K$  bins. The evaluation metrics we report are the average number of  $t = 30$  independent runs, using each time  $N = 500$  different samples.

**Metrics** The evaluation is done with regard to two metrics counting the mean error per bin, where the bin error is defined as the absolute difference of the approximation from the ground-truth. The first metric, Eq. (18), counts the mean bin error wrt average effect and the second, Eq. (19) the mean bin error wrt uncertainty:

$$\mathcal{L}_{\text{DP}|K}^{\mu} = \frac{1}{|\mathcal{Z}^{\text{DP}}|K} \sum_{k \in \mathcal{Z}^{\text{DP}}|K} |\mu(z_k - z_{k-1}) - \hat{\mu}(z_k - z_{k-1})| \quad (18)$$

$$\mathcal{L}_{\text{DP}|K}^{\sigma} = \frac{1}{|\mathcal{Z}^{\text{DP}}|K} \sum_{k \in \mathcal{Z}^{\text{DP}}|K} |\sigma(z_k - z_{k-1}) - \hat{\sigma}(z_k - z_{k-1})| \quad (19)$$

The ground truth  $\mu_k$  ( $\sigma_k$ ) is the mean value of the bin-effects (bin-uncertainties) of the bins inside the interval defined by the wide bin. For better interpretation of the uncertainty error, we also provide the mean (per bin) error term  $\mathcal{L}_{\text{DP}|K}^{\rho} = \frac{1}{|\mathcal{Z}^{\text{DP}}|K} \sum_{k \in \mathcal{Z}^{\text{DP}}|K} \mathcal{E}(z_{k-1}, z_k)$ .

**Piecewise-Linear Function.** In this set-up,  $f(x) = a_1x_1 + x_1x_2$  is a piecewise-linear function with 5 different-width regions, i.e.,  $a_1$  equals to  $\{2, -2, 5, -10, 0.5\}$  in the intervals defined by the sequence  $\{0, 0.2, 0.4, 0.45, 0.5, 1\}$ . As we observe, in Figure 4, UALE’s approximation is better than all fixed-size alternatives, in both mean effect ( $\mathcal{L}^\mu$ ) and uncertainty ( $\mathcal{L}^\sigma$ ). For understanding the importance of variable-size splitting, we analyze the fixed-bin error. In the top-right of Figure 4, we observe the Law of Large Numbers (LLN);  $\mathcal{L}_K^\mu$  and  $K$  have positive correlation because as  $\Delta x$  becomes smaller less points contributing to each estimation. The interpretation of  $\mathcal{L}^\sigma$  is more complex. Given that the smallest piecewise-linear region is  $\Delta x = 0.05$  any  $K$  that is not a multiple of  $\frac{1}{\Delta x} = 20$ , adds nuisance uncertainty  $\mathcal{L}_K^\rho > 0$  leading to a biased uncertainty approximation. For these  $K$ , uncertainty error decreases for bigger  $K$  because the length of the bins that lie in the limit between two piecewise linear regions becomes smaller. For  $K$  that are multiple of 20, i.e.  $K = \{20, 40, 60, 80, 100\}$ , the uncertainty approximation is unbiased  $\mathcal{L}_K^\rho \approx 0$ . Here, as in  $\mathcal{L}^\mu$ , uncertainty estimation is worse as  $K$  grows larger (LLN). As we observe in the top left of Figure 4, automatic bin-splitting separates the fine-grain bins, e.g. regions  $[0.4, 0.45]$ ,  $[0.45, 0.5]$ , and unites constant-effect regions into a single bin, e.g. region  $[0.5, 1]$ .

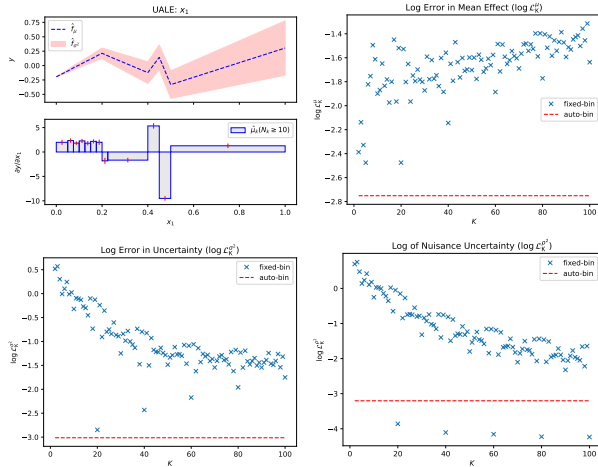


Figure 4: Figure 1

**Non-Linear Function.** In this set-up,  $f(x) = 4x_1^2 + x_2^2 + x_1x_2$ , so the effect is non-linear in  $0 \leq x_1 \leq 1$ . In this set-up, wide bins increase  $\mathcal{L}^{\rho^2}$  making the uncertainty approximation more biased and narrow bins lead to a worse approximation. In Figure 5, we observe that automatic bin splitting manages to compromise the conflicting objectives, [Explain better]

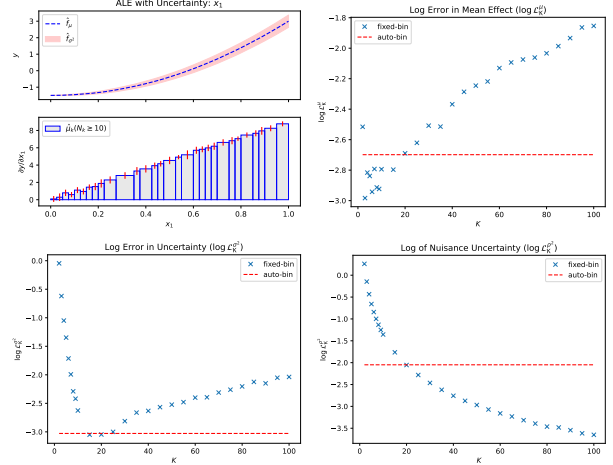


Figure 5: Figure 1

## 5 REAL-WORLD EXAMPLE

Here, we aim at demonstrating the usefulness of uncertainty quantification and the advantages of automatic bin-splitting, on the real-world California Housing dataset (Pace and Barry, 1997).

**ML setup** The California Housing is a largely-studied dataset with approximately 20000 training instances, making it appropriate for robust Monte-Carlo approximations. The dataset contains  $D = 8$  numerical features with characteristics about the building blocks of California, e.g. latitude, longitude, population of the block or median age of houses in the block. The target variable is the median value of the houses inside the block in dollars that ranges between  $[15, 500] \cdot 10^3$ , with a mean value of  $\mu_Y \approx 201 \cdot 10^3$  and a standard deviation of  $\sigma_Y \approx 110 \cdot 10^3$ .

We exclude instances with missing and outlier values. As outlier we define the feature values which are over three standard deviations away from the mean feature value. We also normalize all features to zero-mean and unit standard deviation. We split the dataset into  $N_{tr} = 15639$  training and  $N_{test} = 3910$  test examples (80/20 split) and we fit a Neural Network with 3 hidden layers of 256, 128 and 36 units respectively. After 15 epochs using the Adam optimizer with learning rate  $\eta = 0.02$ , the model achieves a normalized mean squared error (R-Squared) of 0.25 (0.75), which corresponds to a MAE of  $37 \cdot 10^3$  dollars.

Below, we illustrate the feature effect for three features: latitude  $x_2$ , population  $x_6$  and median income  $x_8$ . The particular features cover the main FE cases, e.g. positive/negative trend and linear/non-linear curve, and they are appropriate for illustration purposes. The complete results for all features, along with in-depth information about the preprocessing, training and evaluation parts are provided in the Appendix.

**Uncertainty Quantification** In real-world datasets, it is infeasible to obtain the ground truth FE for seamlessly evaluating the competitive methods. We selected the particular experiment, because, in broad terms, UALE and PDP-ICE plots agree in the estimation of the average effect and uncertainty. Therefore, we can focus on judging the quality of the information provided by the two methods.

In Figure 6, we observe, from top to bottom, the effects for the latitude, population and the median income. The effect of UALE and PDP-ICE are similar for the population and the median income. The population has a negative impact that progressively decreases: from 400 to 1500 people the house value decreases with a rate of  $-150(\pm 140)$  dollars per added person, a rate that decreases from  $-80(\pm 80)$  to  $-60(\pm 60)$  dollars per added person as we move from 1500 to 2800 people. The level of uncertainty indicates significant variance in absolute value of the rate, but in the grant majority of instances the rate is negative. With the same inspection, we observe that the median annual income has a positive impact on the value (all numbers are thousands of dollars):  $20 \pm 15$  per 10 of added median income for incomes in  $[8, 15]$ ,  $32 \pm 20$  per 10 added income in  $[15, 60]$  and  $40 \pm 15$  per 10 added income in  $[60, 70]$ . The uncertainty indicates that there are less heterogeneous effects about the median income compared to the number of people. In both cases, we can end-up to the same conclusion by inspecting the PDP-ICE plots. For the latitude, there is a small difference in the explanations for the region  $[32, 35]$ , where UALE estimates a less negative slope with less uncertainty than PDP, while the explanations are similar for the range  $[35, 39]$ , where both methods reveal an increase in the uncertainty around the feature value 37.5.

In general, we observe that UALE complements ALE in the quantification of the heterogeneous effects, similarly to as ICE complements PDP. The automatic extraction of constant-effect and constant-uncertainty regions provided by UALE is helpful for an easier interpretation. On the other hand, ICE plots sometimes are more descriptive on locating the type of heterogeneity, whereas UALE quantifies only the level (not the type) of heterogeneity.

**Bin Splitting** In this part, we evaluate the robustness of the approximation using automatic bin-splitting. Following the evaluation framework of Section 4.2, we treat as ground-truth the effects computed on the full training-set  $N = 20000$  with dense fixed-size bin-splitting ( $K = 80$ ). Given the big number of samples, we make the hypothesis that the approximation with dense binning is close to the ground truth. Afterwards, we randomly select less samples  $N = 1000$  and we compare UALE approximation with all possible fixed-size alternatives, repeating this process for 30 times for robust results. In Figure 7, we illustrate the mean values for  $\mathcal{L}^\mu$ ,  $\mathcal{L}^\sigma$  of the 30 repetitions. We observe that automatic bin-splitting provides (close to the) best ap-

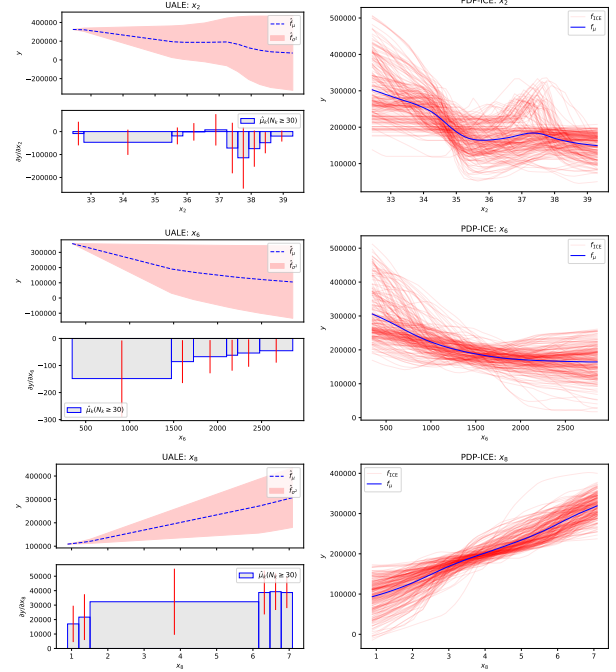


Figure 6: Figure 1

proximation in the three features. In the Appendix, we provide the same evaluation for all features.

## 6 DISCUSSION

[Add Conclusion, limitations, and future work]

### Acknowledgments

All acknowledgments go at the end of the paper, including thanks to reviewers who gave useful comments, to colleagues who contributed to the ideas, and to funding agencies and corporate sponsors that provided financial support. To preserve the anonymity, please include acknowledgments *only* in the camera-ready papers.

### References

- Kjersti Aas, Martin Jullum, and Anders Løland. Explaining individual predictions when features are dependent: More accurate approximations to shapley values. *Artificial Intelligence*, 298:103502, 2021.
- Daniel W Apley and Jingyu Zhu. Visualizing the effects of predictor variables in black box supervised learning models. *Journal of the Royal Statistical Society: Series B (Statistical Methodology)*, 82(4):1059–1086, 2020.
- Hubert Baniecki, Wojciech Kretowicz, and Przemysław Biecek. Fooling partial dependence via data poisoning. *arXiv preprint arXiv:2105.12837*, 2021.



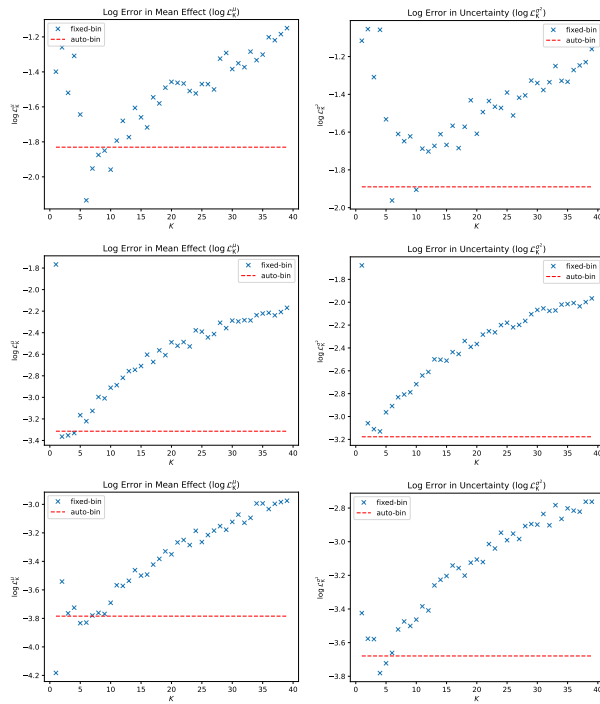


Figure 7: Figure 1

- Scott M Lundberg, Gabriel G Erion, and Su-In Lee. Consistent individualized feature attribution for tree ensembles. *arXiv preprint arXiv:1802.03888*, 2018.
- Ninareh Mehrabi, Fred Morstatter, Nripsuta Saxena, Kristina Lerman, and Aram Galstyan. A survey on bias and fairness in machine learning. *ACM Computing Surveys (CSUR)*, 54(6):1–35, 2021.
- Christoph Molnar. *Interpretable Machine Learning*. 2 edition, 2022. URL <https://christophm.github.io/interpretable-ml-book>.
- Christoph Molnar, Giuseppe Casalicchio, and Bernd Bischl. Interpretable machine learning—a brief history, state-of-the-art and challenges. In *Joint European Conference on Machine Learning and Knowledge Discovery in Databases*, pages 417–431. Springer, 2020a.
- Christoph Molnar, Gunnar König, Bernd Bischl, and Giuseppe Casalicchio. Model-agnostic feature importance and effects with dependent features—a conditional subgroup approach. *arXiv preprint arXiv:2006.04628*, 2020b.
- R Kelley Pace and Ronald Barry. Sparse spatial autoregressions. *Statistics & Probability Letters*, 33(3):291–297, 1997.
- Matthew Britton. Vine: visualizing statistical interactions in black box models. *arXiv preprint arXiv:1904.00561*, 2019.
- Jerome H Friedman. Greedy function approximation: a gradient boosting machine. *Annals of statistics*, pages 1189–1232, 2001.
- Jerome H Friedman and Bogdan E Popescu. Predictive learning via rule ensembles. *The annals of applied statistics*, pages 916–954, 2008.
- Vasilis Gkolemis, Theodore Dalamagas, and Christos Diou. Dale: Differential accumulated local effects for efficient and accurate global explanations.
- Alex Goldstein, Adam Kapelner, Justin Bleich, and Emil Pitkin. Peeking inside the black box: Visualizing statistical learning with plots of individual conditional expectation. *journal of Computational and Graphical Statistics*, 24(1):44–65, 2015.
- Brandon M Greenwell, Bradley C Boehmke, and Andrew J McCarthy. A simple and effective model-based variable importance measure. *arXiv preprint arXiv:1805.04755*, 2018.
- Ulrike Grömping. Model-agnostic effects plots for interpreting machine learning models, 03 2020.
- Julia Herbringer, Bernd Bischl, and Giuseppe Casalicchio. Repid: Regional effect plots with implicit interaction detection. In *International Conference on Artificial Intelligence and Statistics*, pages 10209–10233. PMLR, 2022.